Hindawi
Advances in Materials Science and Engineering
Volume 2023, Article ID 5487193, 15 pages
https://doi.org/10.1155/2023/5487193

Research Article

Effect of Load on Tribological Characteristics of H-AlSi24Cu3.8Mg0.8 Alloy Under Dry, Lubricated, and Coated (a–c: H) Sliding Conditions

M. Peeru Naik,[1] K. T. Balaram Padal,[1] and Muralidhar Avvari [2]

[1]*Department of Mechanical Engineering, Andhra University, Visakhapatnam, Andhra Pradesh, India*
[2]*Faculty of Mechanical Engineering, AMiT Arba Minch University, Arba Minch, Ethiopia*

Correspondence should be addressed to Muralidhar Avvari; muralidhar.avvari@amu.edu.et

Received 4 September 2022; Revised 15 October 2022; Accepted 25 November 2022; Published 27 January 2023

Academic Editor: Samson Jerold Samuel Chelladurai

This paper presents the new route of fabrication of H-AlSi24Cu3.8Mg0.8 alloy, assisted by ultrasonic vibration stirring and squeeze casting (UVSS). The primary objective of this investigation is to establish the tribological characteristics of the prepared aluminium alloy under dry, lubricated, and coated sliding conditions. Oil SAE20W40 is used as a lubricant and diamond-like carbon (DLC) is used as a coating. Under a load between 20 N and 50 N, a linear reciprocating tribometer (LRT) with a ball-on-plate geometry is used. Alloy was examined using an optical microscope, scanning electron microscope with EDS, 3D surface profilometer, Brinell hardness tester, and tensometer for pre- and postcharacterization of alloy, surface, and worn tracks. The DLC-coated condition yields the lowest wear and coefficient of friction.

1. Introduction

Among aluminium alloys, aluminium-silicon (Al-Si) alloys are light-weight materials with excellent properties such as good castability, high wear resistance, high corrosion resistance, low thermal expansion, good thermal conductivity, and superior mechanical properties [1–3]. The Al-Si alloys are categorized into three types based on wt. % of silicon, i.e., (1) hypoeutectic (<10), (2) eutectic (10–13), and (3) hypereutectic (>13). Among them, hypereutectic Al-Si alloys exhibit great potency in various applications such as automobiles, aerospace, electronics, and optics [4, 5]. Hypereutectic Al-Si alloys are very promising in automobile applications, i.e., pistons, compressor cylinders, propeller casings, rims, and disc brakes, due to their low thermal expansion and high wear resistance due to the presence of primary Si particles (PSP) [6, 7]. Thermal resistance, high specific strength, abrasion resistance, and corrosion resistance are only a few of the properties of Al-Si composites [8, 9].

However, the tribological characteristics of Al-Si alloys are dependent on the wt. % and size of Si particles and the method of production. Reddy et al. investigated the variation in wt. % of Si in the Al-Si alloy and observed an increase in wear resistance of the alloy with the increase in wt. % of Si. Besides the increase in wt. % of Si, fabricating the Al-Si alloys by the conventional casting routes forms coarser and brittle Si particles in the form of thick needles, which reduces the mechanical strength and exhibits poor tribological characteristics such as the coefficient of friction and wear rate of the components at elevated or working temperatures.

Researchers developed and investigated various routes such as ultrasonic vibration [10, 11], powder metallurgy, and rapid solidification techniques, i.e., spray deposition, planar flow casting, selective laser melting, and high-pulse electron beam, to refine the Si particles in the Al matrix and improve the wear resistance of the alloy. Researchers investigated the impact of stir-squeeze casting on the tribological characteristics of hybrid aluminium matrix composites and observed a significant enhancement in the friction and wear

resistance of the hybrid composite [12–17] compared with the sand and stir casting. A relatively innovative way of stirring and squeezing Al-Si composites is the use of ultrasonic vibration. User-friendly, low-cost, and easy-to-use are only a few of the advantages of this expertise. The tribological characteristics of hybrid aluminium matrix composites were studied by Edacherian et al. and Khemraj Stir-squeeze casting significantly enhanced the hybrid composite [18, 19] according to the researchers. The Al-Si composite's wear-resistance properties are improved by the inclusion of Si-like hard particles [20] under wet and dry lubrication, Kumar and Wani used an LRT to investigate the wear behavior of an AlSi25 composite (linear reciprocating tribometer). Lubricating oil (SAE20W40) was shown to have a significant impact on COF and wear coefficient in this research [21]. To keep up with today's more powerful automobiles, however, newer, more powerful vehicles need lubricants that can resist tremendous loads and temperatures for a lengthy period of time.

Nevertheless, the search for a lubricant with the least tribological qualities is currently ongoing aside from their corrosion resistance, hardness, and thermal stability, these coatings (DLC) also have remarkable tribological qualities [22, 23]. Apart from type of reinforcement and method of production, lubrication also plays a major role in reduction of friction and wear rate of components. The selection of the proper lubricant is a crucial factor in automotive applications. Parveen Kumar et al. investigated the tribological behavior of AlSi25 MMC under lubricated and dry conditions and observed that with lubricating oil (SAE20W40) significantly reduced C. O. F and wear coefficient [24]. .Researchers have also noticed that in high load wear experiments with lubrication, Si-particles that are mixed with the lubricating fluid and jut out from the matrix operate as a solid lubricant to greatly lower the coefficient of friction and the rate of wear. [25].

Diamond-like carbon is an energetic material that has been extensively studied for its wide range of tribological and mechanical properties (DLC). Aside from their corrosion resistance, hardness, and thermal stability, these coatings (DLC) also have remarkable tribological qualities. In contrast, the tribological performances of a–C: H coatings for Al alloys under ambient conditions are superior to those of other coatings, such as CrN and TiN. The friction coefficient (0.001–003) was significantly reduced, and the wear rate (10-10-10-11 mm^3/Nm) was significantly improved by DLC coatings on aluminium alloys in inert gas and dry nitrogen environment [23, 24, 26–31]. Wear scars get deeper, larger and softer at increased temperatures when researchers perform studies on a–C: H films [32]. Good adhesion was obtained by surface decarburization of the substrate before diamond coating [33]. The wear mechanism of CVD diamond inserts in machining high-silicon aluminium alloys [34, 35]. Drilling of hypereutectic Al-Si alloys with the H-DLC-coated drills led to shortened tool lives characterized by flank wear as the primary Si particles removed the H-DLC coating and increased friction and wear [36]. E-MRS spring meeting was from June 2 to 5 in Strasbourg, France [37]. The development of the alloys from ancient to present time initiated from accidents to through the use of well-defined scientific principles [38]. A DLC coating has been shown in these investigations to have exceptional hard film properties for fighting coefficients of friction and wear rates in several tribological applications. The tribological features of Al-Si composites are clearly dependent on the production method and the amount of Si present [39, 40]. The surface morphology was also studied to infer the basic mechanisms involved during composite machining [41]. The objective of this investigation was to study the effect of surface modifications (NaOH & H_2SO_4) on mechanical properties, including tensile, shear, and impact strengths [42].

It is inferred from the literature, ultrasonic vibration assisted stir casting is an innovative, easy-to-use, and economical technique to produce components with any shape and dimensions as compared with the other conventional and advanced techniques. Lubricant SAE20W40 significantly reduces the coefficient of friction and wear friction of Al-Si alloys. Diamond-like carbon coating exhibits excellent tribological characteristics and thermal stability. In the present investigation, the prime objective is to study the tribological characteristics of UV-assistedstir-squeeze cast alloys under dry, lubricated, and coated conditions and compare the performances individually.

2. Materials and Methods

2.1. Preparation of Alloys and Specimens. In the present study, the alloy was prepared by a new route of fabrication, i.e., ultrasonic vibration-assisted stirring and squeeze casting (UVSS), as shown in Figure 1. The major components of the equipment are (i) a furnace with a stirrer, (ii) a squeeze casting setup, (iii) an ultrasonic vibration (UV) generator, and (iv) a titanium alloy horn. This UV test made use of a frequency of 20 kHz and a maximum power output of 2.8 kW.

A hypereutectic AlSi24Cu3.5–4Mg0.6–0.8 (H-AlSi24) alloy was prepared using pure aluminium, copper plates, and silicon and magnesium powder procured from the reputed metal suppliers in the market. The complete procedure is divided into two stages, i.e., (i) preparation of the master alloy and (ii) squeeze casting into ingot. In the first stage, the required wt. % of Al, Cu, Si, and Mg was preheated at 250°C for 30 min in a muffle furnace (Figure 1(b)) to remove the moisture or absorbed gases on the plate/particle surface to avoid oxidation. After preheating, the Al and Cu plates are placed in a graphite crucible and heated to a liquid state at 1100°C using a gas furnace, and then the mixture is slowly brought to 720°C and stirred mechanically for 10 min. The preheated Si and Mg powders were divided into three batches and added to the melt and stirred at 300 rpm for equal intervals of 05 mins. After stirring, the mixture is again brought to 1100°C, and an ultrasonic vibration is applied for 05 mins using a titanium alloy horn to disperse the Mg and Si particles uniformly throughout the matrix. It is then transferred into a preheated (200°C) H13 die steel mold. In stage two, a pressure of 150 MPa was applied at top and bottom with a holding time of 60 s to obtain a rapidly solidified square casting

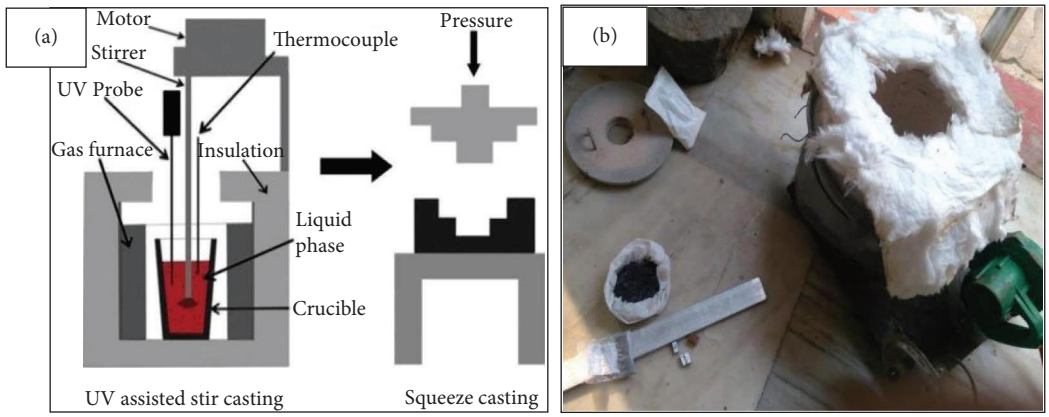

Figure 1: (a) Schematic setup and (b) muffle furnace.

billet of $40 \times 40 \times 100$ mm. Furthermore, the alloy is applied to a hardening treatment (*T*6), i.e., heating the billets in muffle furnace at 500°C for 4 hours and then rapidly quenching to water at 50°C; later, the alloys were artificially aged at 165°C for 4 hours in muffle furnace and then air cooled to room temperature.

2.2. Diamond-Like Carbon (DLC) Coating. After preparation of the final alloy in two stages, the alloys are cut into samples of 10 mm thickness and coated with DLC, i.e., hydrogenated amorphous carbon (a–C: H) of 4 μm thickness Figure 2 to determine the tribological characteristics. The coating technology used is plasma-assisted chemical vapor deposition (PACVD) and deposited at 250°C supplied by Oerlikon Blazers.

2.3. Tribological Tests. To determine and evaluate the tribological characteristics of the prepared alloy under various conditions, a linear reciprocating tribometer (LRT) by DUCOM Ltd., was employed in the present investigation. A 6 mm dia. ball-on-a-square plate geometry was selected and used to perform wear and friction testing at room temperature, as shown in Figure 3. The consisting of weight of samples before and after wear test in Table 1.

The investigation was carried out in three sliding conditions, as shown in, i.e., Table 2 [24].

A frequency of 30 Hz was used with a load range of 20–50 N for the friction and wear test. The sliding distance was 80 m and the stroke length was 2 mm, therefore the reciprocating experiment lasted 15 minutes. After that, the LRT display was used to acquire the values of friction coefficients, and the following equation was used to compute the alloys' wear coefficients (kw) and the equation (1) is as follows:

$$\text{Wear coefficient (kw)} = \frac{\text{Wear volume}}{(\text{Applied Load X Slidi ng di atance})} \frac{\text{mm}^3}{\text{N.m}}, \quad (1)$$

where the applied load is denoted as F_n (N), sliding distance is denoted as S_d (m), and wear volume is denoted as W_v (mm^3).

2.4. Characterization. After casting, heat treatment and wear tests the alloys were examined to study the microstructure, morphology and hardness. Samples of as cast and heat treated were mechanically polished using various grades of emery sheets, i.e., 80–2000 grit and then wet polished using diamond paste to obtain mirror finish. After polishing the samples were cleaned with benzene followed by acetone to remove any residues present on the surface, and then etched with a suitable etchant. Samples were exposed under Brinell hardness tester with a load of 250 kgf and ball diameter of 5 mm (ASTM E10-15) to determine the hardness of the prepared alloy. The sample were also examined under optical microscope (Figure 4) and scanning electron microscope with energy dispersive spectroscopy (SEM—EDS) (Figure to capture microstructure and morphology of the alloys before and after the experimentation. A 3D Profilometer is used to assess the surface topography of the alloy after the wear tests. Also, the prepared alloys are evaluated for tensile properties according to ASTM E8/E8M using a tensometer of 20 N, and the dimensions of the specimen are shown in Figure 4.

3. Results and Discussion

3.1. Elemental Composition of the Alloy. After preparation of final alloy, the actual elemental composition was determined by using optical emission spectrometer, and tabulated in Table 4.

3.2. Microstructure and Morphology of the Alloy. Figure 5(a) shows the optical micrograph, and Figure 5(b) shows the secondary electron image of the alloy, and both the images clearly reveal the presence of Si granules in the matrix. Figure 5(c) shows EDS spectrum of the alloy and confirms the Si granules in Al matrix.

The microstructural study of a material can provide information regarding the morphology and distribution of constituent phases as well as the nature and pattern of certain crystallographic imperfections. A limited study of line and surface information is also possible with the optical microscope. In order to obtain reproducible results with good contrast in the image, the specimen surface is polished and

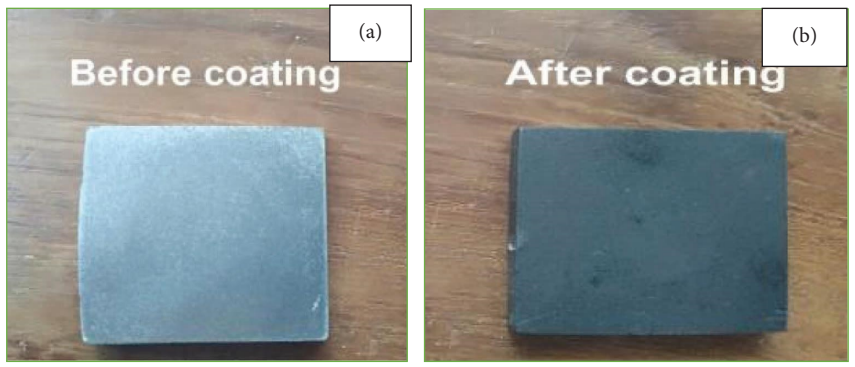

Figure 2: Alloy (a) before coating and (b) after coating.

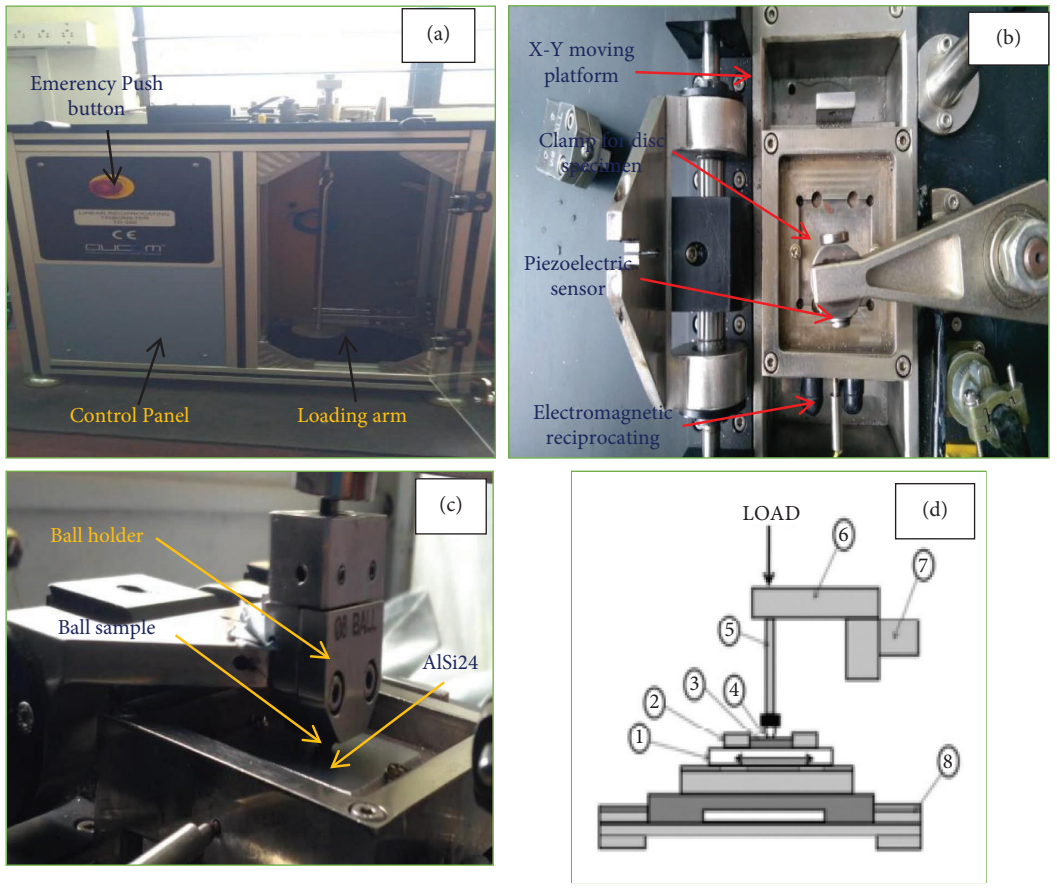

Figure 3: (a–c) Linear reciprocating tribometer test set up and (d) schematic of set up. (1) Electromagnetic reciprocating drive. (2) Clamp for disc specimen. (3) Disc sample. (4) Ball sample. (5) Ball holder. (6) Loading arm. (7) Piezoelectric sensor. (8) *X-Y* moving platform.

subsequently etched with appropriate reagents before microscopic examination. In a polished specimen, the etching not only delineates grain boundaries but also allows the different phases to be distinguished by differences in brightness, shape, and color of the grain. Grain boundaries are often anodic to the bulk metal in the interior of the grain, and so are etched away preferentially and delineated. Staining is produced by the deposition of a solid etch product on the specimen surface. This is formed by a chemical reaction between the etchant and the specimen. Under favorable conditions the use of a proper etchant enables the identification of constituents. Microstructural examination can provide quantitative information about the following parameters:

(1) The grain size of specimens
(2) The amount of interfacial area per unit volume
(3) The dimensions of constituent phases
(4) The amount and distribution of phases.

3.3. Hardness and Tensile Test. The prepared alloy was examined before and after heat treatment under Brinell

Table 1: Weight of samples before and after wear test of AlSi24 composite.

S. no	Alloys	Initial mass (g)	Final mass (g)	Mass loss (g)
1	Dry (20 N)	42.70955	42.70955	0
2	Dry (30 N)	43.52535	43.52533	0.00002
3	Dry (40 N)	43.41546	43.41538	0.00008
4	Dry (50 N)	43.13754	43.13733	0.00021
5	Coated (20 N)	42.70965	42.70965	0
6	Coated (30 N)	43.70955	43.70954	0.00001
7	Coated (40 N)	43.70965	43.70962	0.00003
8	Coated (50 N)	42.70945	42.70942	0.00003
9	Lubricated (20 N)	42.70955	42.70955	0
10	Lubricated (30 N)	43.52535	43.52535	0
11	Lubricated (40 N)	43.41546	43.41545	0.00001
12	Lubricated (50 N)	43.13754	43.13754	0

Table 2: Various conditions tested for the Al-Si alloy.

S. no	Condition	Description
1	Dry	Al-Si composite against steel ball
2	Lubricated	Al-Si alloy against steel ball under the oil medium SAE20W40 oil used as lubricant and the properties are tabulated in Table 3
3	Coated	DLC coated Al-Si composite against steel ball

Table 3: Properties of lubricant oil grade SAE20W40.

Lubricant properties	Value
Viscosity @100°C, mm^2/s	14.0
Viscosity index	115
Flash point	230°C
Pour point	−21°C

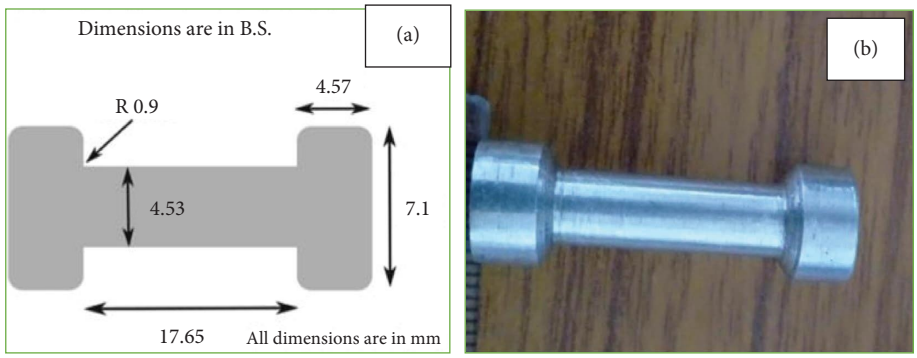

Figure 4: (a) Dimensions (b) specimen for test.

Table 4: Elemental composition of alloy.

Alloy	Al	Si	Cu	Mg
AlSi24Cu3.8Mg0.8	Balance	24	3.8–4	0.6–0.8

hardness tester at room temperature and the results are tabulated in Table 5 and alloys in Figure 6. The study values of Figure 7 show that the hardness of the AlSi24 composite is improved for UVSS-T6 manufactured samples.

The tensile strength of the alloys is determined using tensometer and the results are tabulated in Table 6 and Figure 8 Images represent that the UVSS-T6 technique leads to superior strengthening effects for AlSi24 composite.

3.4. Coefficient of Friction. The coefficient of friction is a function of the applied load, and Figure 9 depicts the same under dry, lubricated, and coated conditions of wear test. It is observed that as the load increases from 20 N to 50 N the

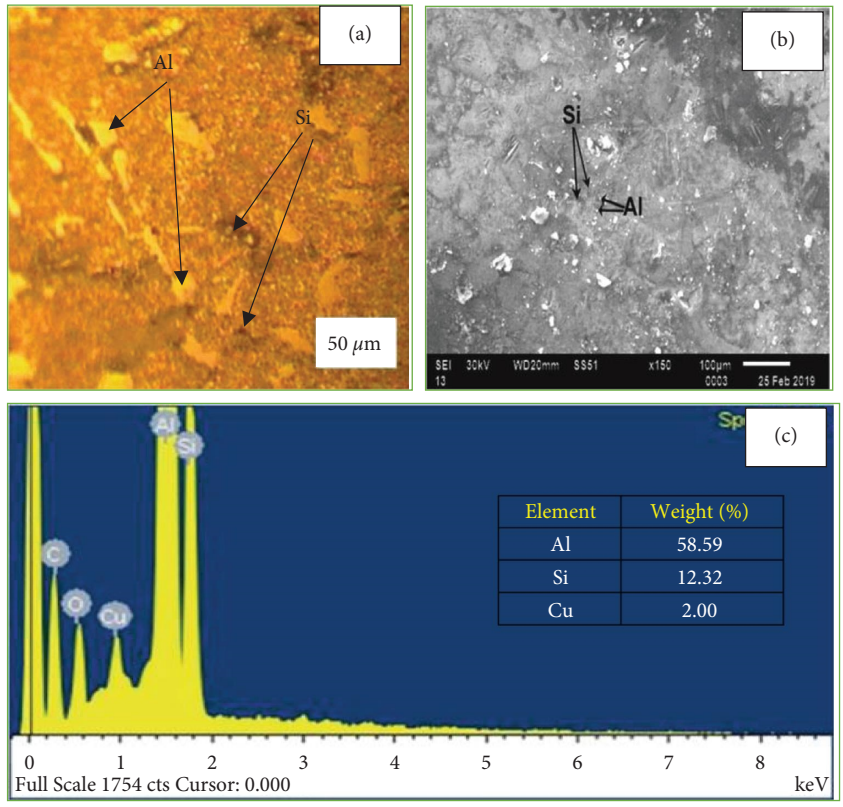

Figure 5: (a) Microstructure, (b) morphology, and (c) EDS spectrum.

Table 5: Hardness values of AlSi24 composite.

Composition	Load (kgf)	Ball diameter (mm)	Hardness value before heat treatment (BHN)	Hardness value after heat treatment (BHN)
AlSi24	250	5	104.51	162.94

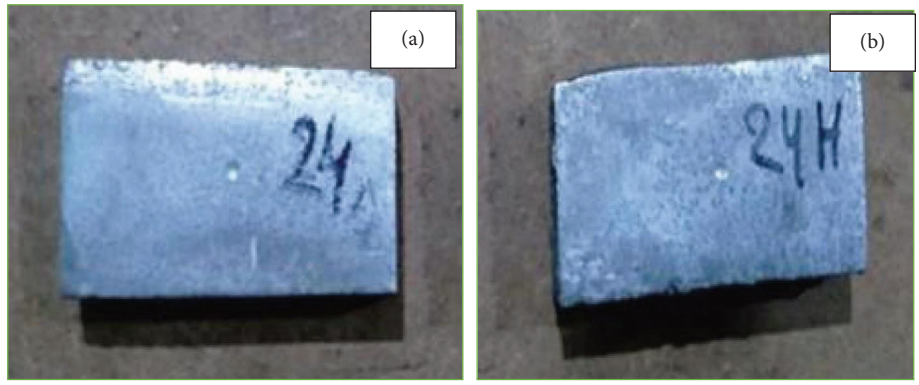

Figure 6: Hardness test alloys (a) AlSi24 (UVS) and (b) AlSi24 (UVSS-T6).

C. O. F decreases in all the three conditions. The C. O. F of tribopair is higher, moderate, and lower at dry, lubricated, and DLC coated conditions, respectively. The C. O. F under the lubricated condition declines from 0.082 to 0.039 at 20 N and 50 N, respectively, i.e., a reduction of about 47.5% and confirms that SAE20W40 lubricant significantly reduced the COF as compared to the dry condition.

The reduction attributes to the following mechanisms: (i) formation of thin oil film acts as coolant and reduces friction between the tribopair and (ii) an increase in load releases the hard Si particles in the alloy matrix mixed with lubricating oil which acts as a solid lubricant.

The DLC-coatedAl-Si alloy results in the very lowest C. O. F, i.e., 0.011 at 50 N compared to lubricated and dry

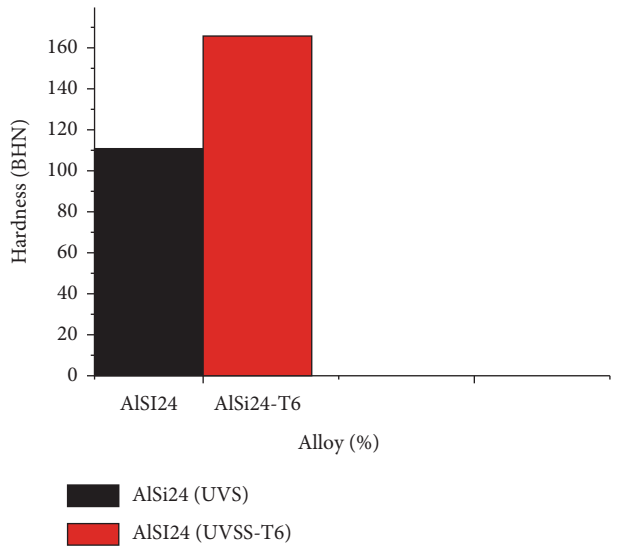

Figure 7: Hardness values of AlSi24 alloy.

Table 6: Tensile properties of AlSi24 composite.

Composition	UTS RSSC-T6	YS RSSC-T6	Elongation (%) RSSC-T6
AlSi24	387	369	0.8

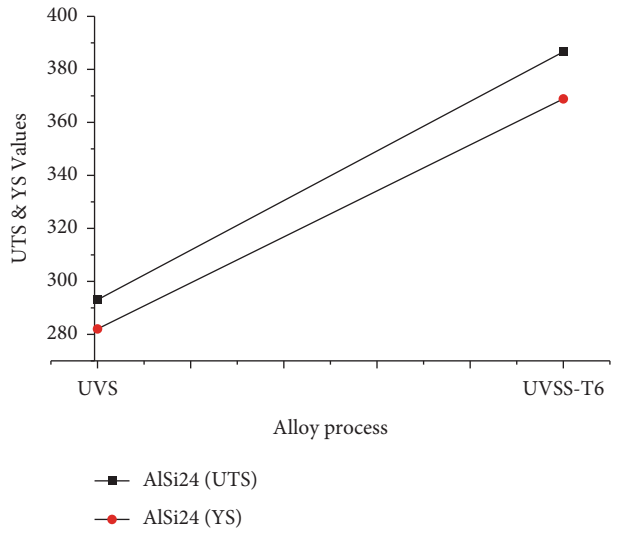

Figure 8: UTS and YS values of AlSi24 alloy.

sliding conditions, with a reduction of 45.8%. The reduction in C. O. F attributes to (i) refinement of Si particle and (ii) formation of tribo-oxidation coatings between the mating components.

3.5. Analysis of Wear. The wear coefficient of the prepared and tested H-AlSi4 alloy under dry, lubricated, and coated test conditions are shown in Figure 10. After testing, results reveal that $AlSi_{24}$ achieved a highest wear coefficient of 3.2×10^{-3} mm^3/Nm, 3.5×10^{-4} mm^3/Nm, and 4.4×10^{-5} mm^3/Nm at 20 N in dry, lubricated, and coated conditions, respectively. It is also observed that the dry condition yields the highest wear coefficient and the coated condition yields a very low wear coefficient.

After wear tests, the alloys (sample discs) were examined an under optical microscope and a scanning electron microscope to capture the morphology of the alloy and evaluate the type of wear and its roots.

Figure 11 shows the optical micrographs and secondary electron images of the worn surfaces of an alloy (sample disc) under dry conditions. At 20 N load, due to the reciprocating

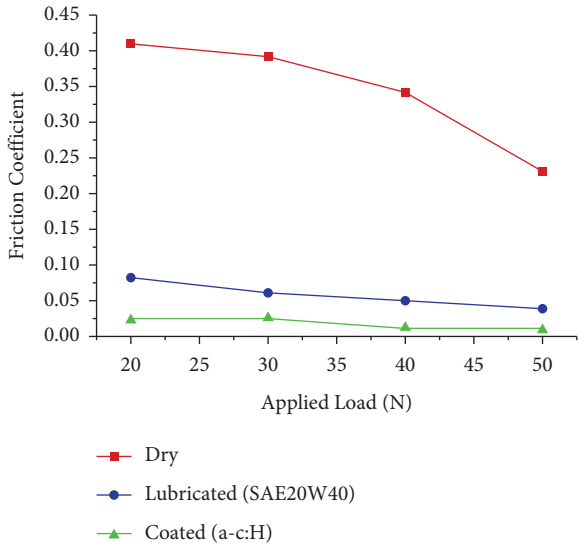

Figure 9: Effect of load vs. coefficient of friction.

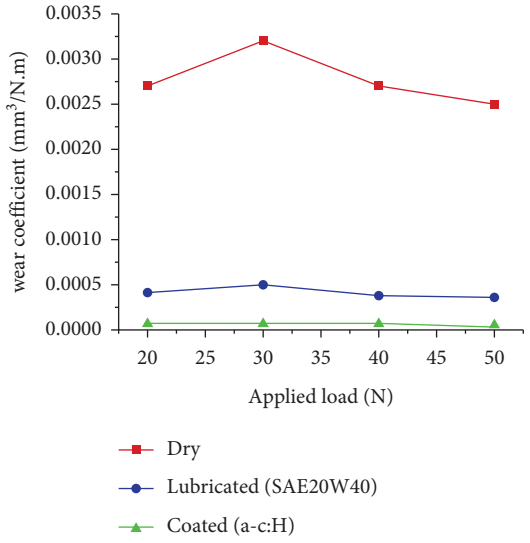

Figure 10: Effect of load vs. wear coefficient.

motion, a small groove (Figures 11(a) and 11(e)) forms between the tribopair which indicates an abrasive wear, and an increase in load to 30 N breaks the particles like Al, Si, and Fe from the surface of the sample disc (red colored zones i.e., Figures 11(b) and 11(f)) and transfers them to the surface of the steel ball and adheres.

The adhesion of particles and reciprocating motion combinedly forms deep rubbing scratches, i.e., abrasive and adhesive wear. Further increase in load to 40 and 50 N reveals a smooth surface (Figures 11(g) and 11(h)) due to the jutted-out Si particles forms oxide layer and reduces the friction confirms from the Figures 9 and 10. It is evident from the information provided above that adhesion, abrasion, and the creation of thin oxide layers were the most effective wear mechanisms under dry circumstances.

The wear coefficient (Figure 10) was significantly reduced under SAE20W40 oil lubricant environment as compared to a dry condition. Figure 12 shows the optical micrographs and secondary electron images of the worn surfaces of alloy (sample disc) under lubricated conditions. The surface of the sample disc under 20 N (Figures 12(a) and 12(e)) displays minor wear tracks with a substantial wear scar due to the thin lubricating film between the tribo pair.

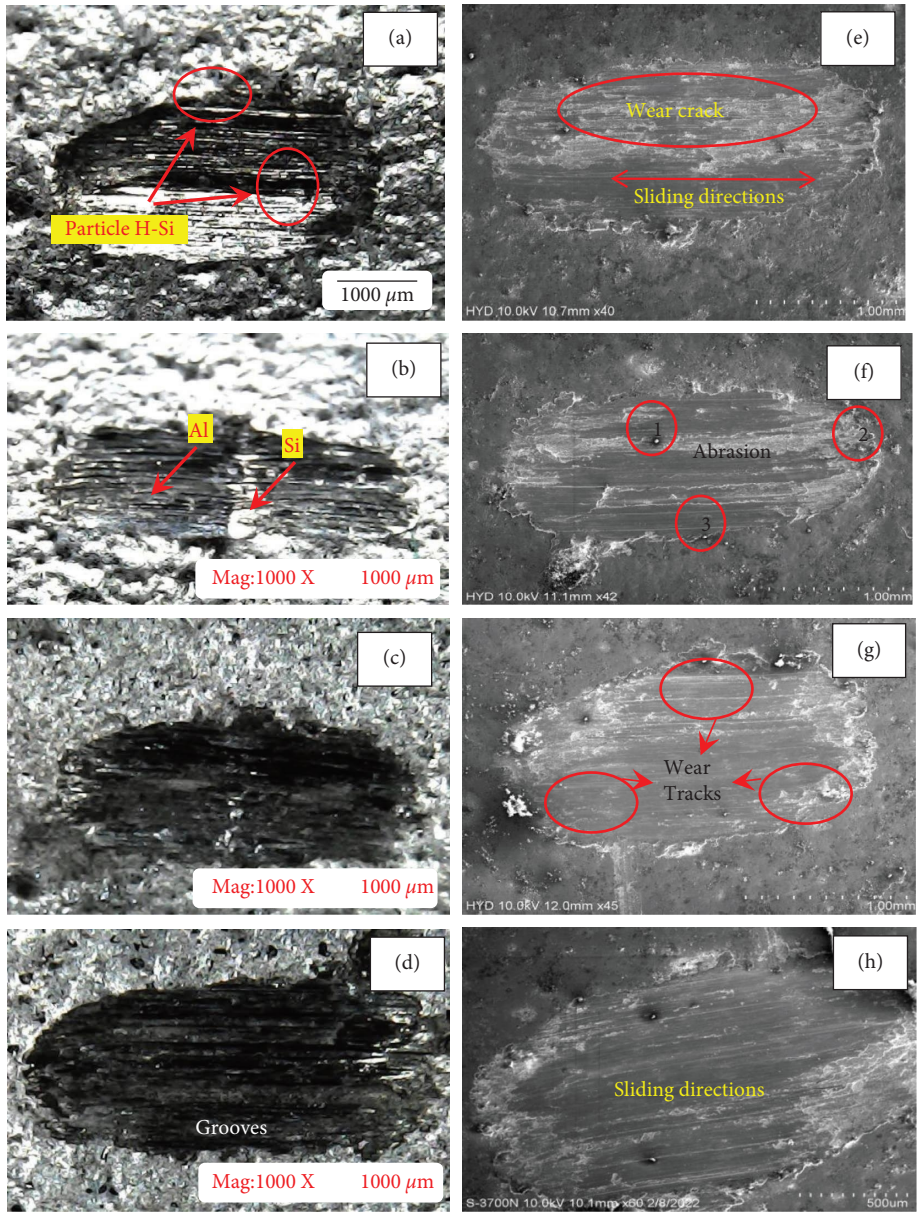

Figure 11: Micrographs of HAlSi24 under dry conditions at (a) 20 N, (b) 30 N, (c) 40 N, and (d) 50 N load. Morphology of HAlSi24 under dry conditions at (e) 20 N, (f) 30 N, (g) 40 N, and (h) 50 N load.

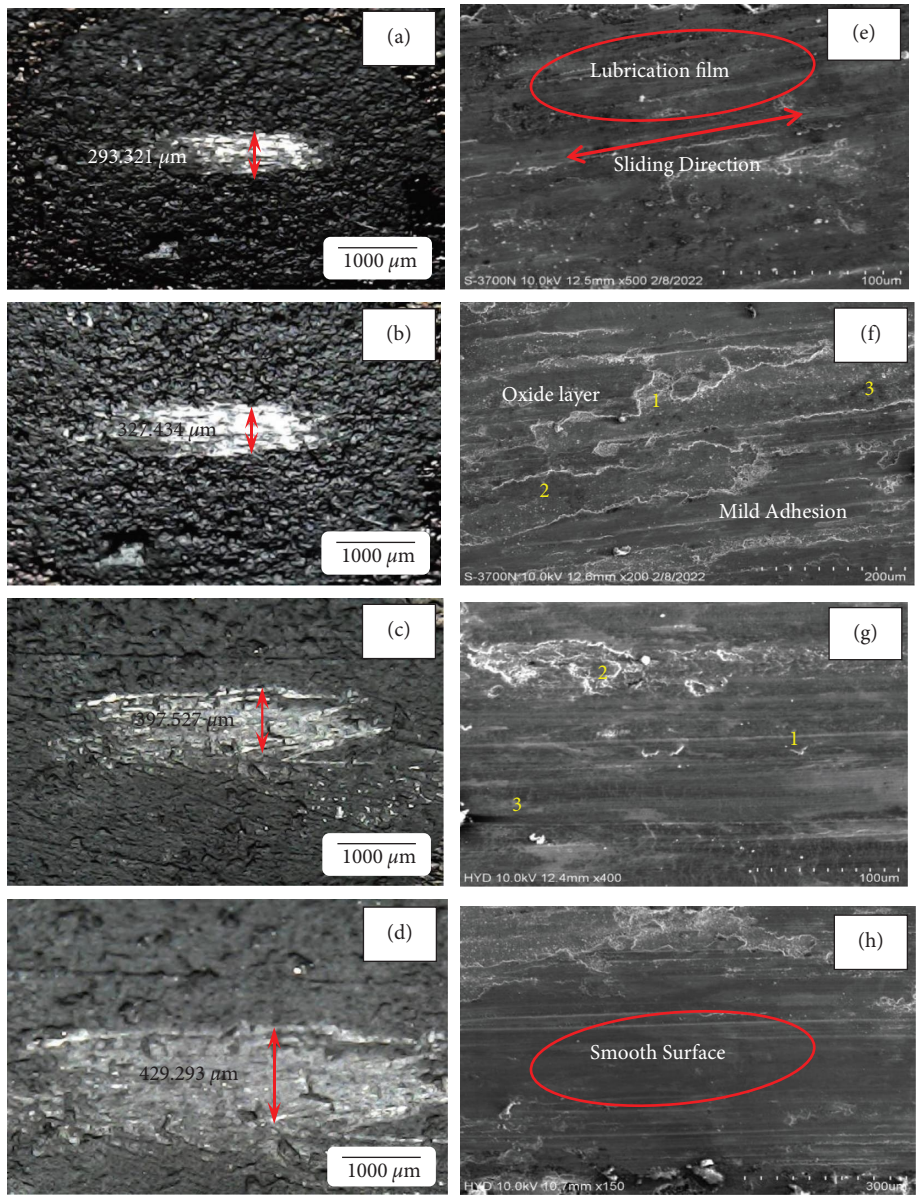

Figure 12: Micrographs of HAlSi24 under lubricated condition at (a) 20 N, (b) 30 N, (c) 40 N, and (d) 50 N. Morphology of HAlSi24 under lubricated conditions at (e) 20 N, (f) 30 N, (g) 40 N, and (h) 50 N.

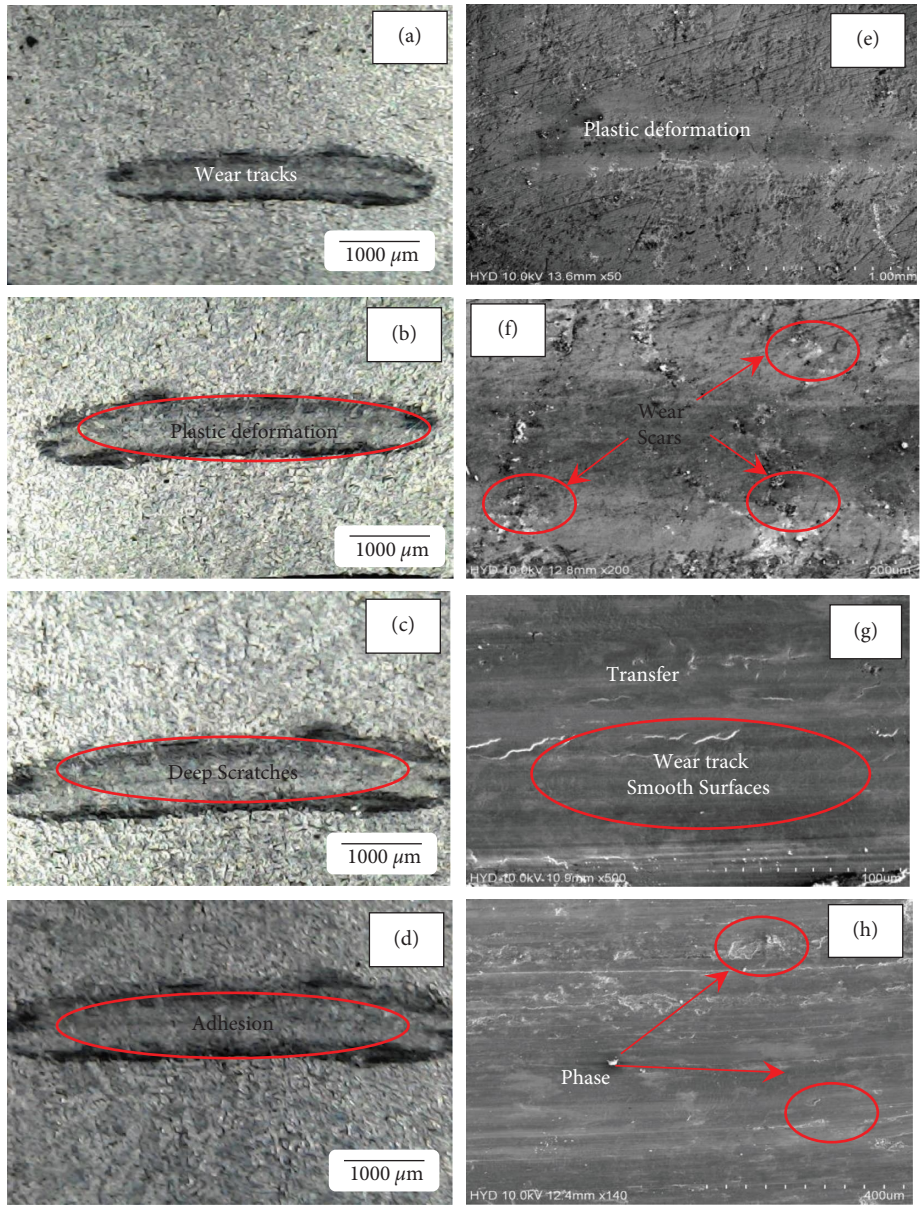

Figure 13: Micrographs of HAlSi24 under DLC-coated condition at (a) 20 N, (b) 30 N, (c) 40 N, and (d) 50 N. Morphology of HAlSi24 under DLC-coated conditions at (e) 20 N, (f) 30 N, (g) 40 N, and (h) 50 N.

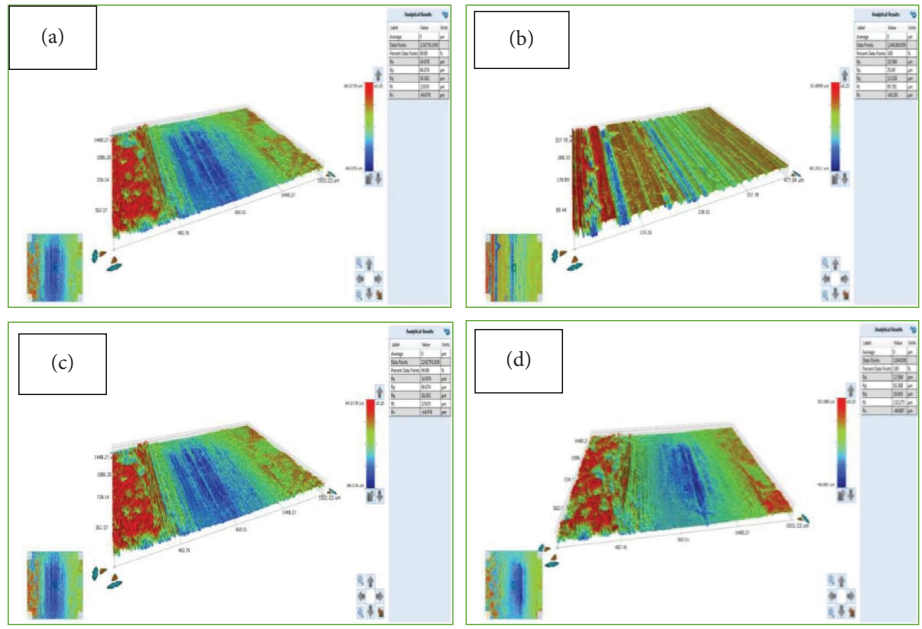

Figure 14: Surface topography of alloy under dry condition at (a) 20 N, (b) 30 N, (c) 40 N, and (d) 50 N.

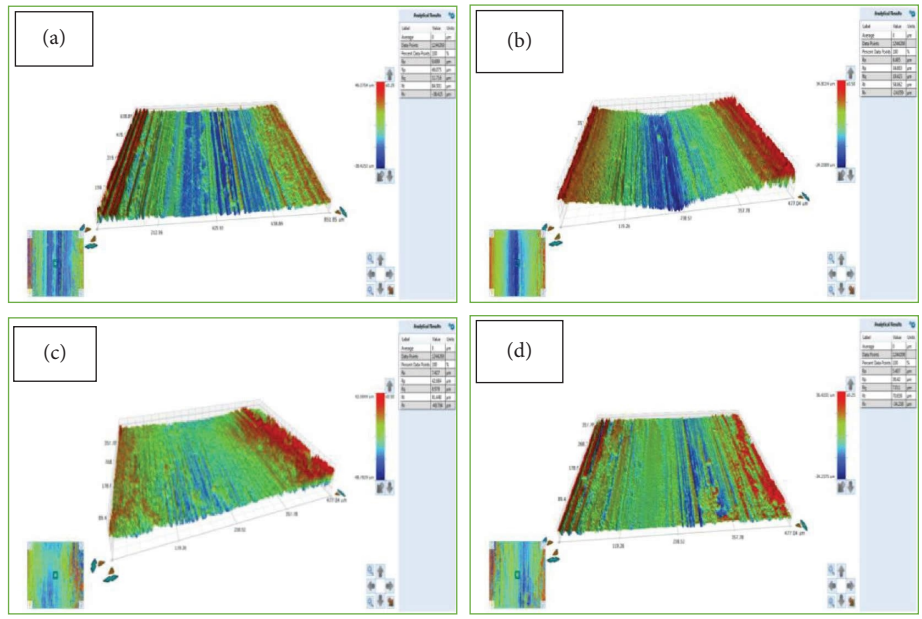

Figure 15: 3D profilometer image of HAlSi24 alloy under lubricated condition at (a) 20 N, (b) 30 N, (c) 40 N, and (d) 50 N.

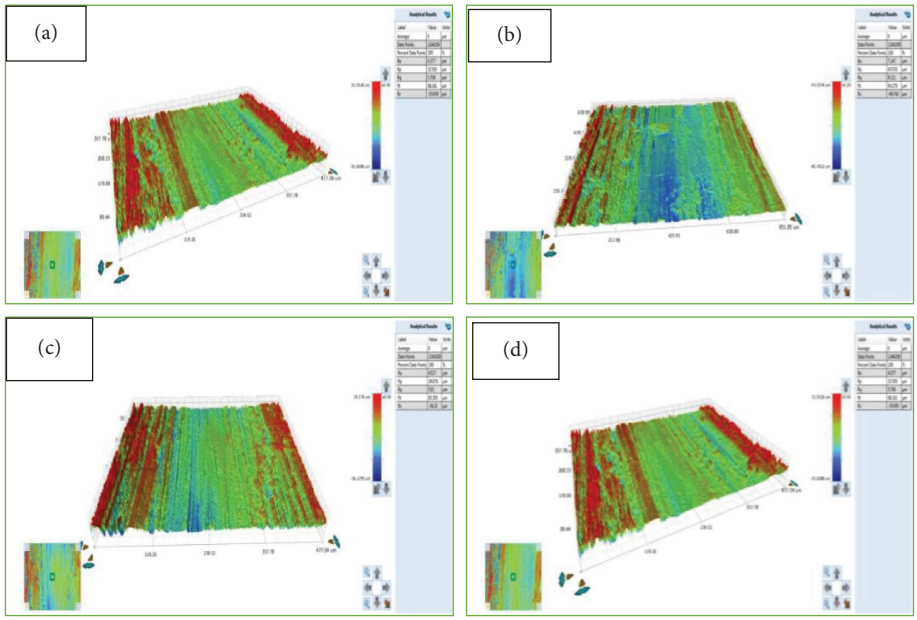

Figure 16: 3D profilometer image of HAlSi24 alloy under DLC coated condition at (a) 20 N, (b) 30 N, (c) 40 N, and (d) 50 N.

An increase in load to 30 N causes a little adhesion of abrasives to the steel ball resulting in a little increase on wear coefficient (Figures 12(b) and 12(f)). When the load is increased further to 40 N and 50 N, the Si particles/granules mixes with the lubricating oil and form a solid lubricant that creates a smooth surface (Figure 12(h)).

The wear coefficient of the alloy was drastically decreased under DLC-coated condition (Figure 10) as compared to both lubricated and dry environments. Figure 13 shows the optical micrographs and secondary electron images of the worn surfaces of alloy (sample disc) under DLC-coated conditions. DLC coat has a greater surface polish and yields almost zero wear coefficient at 20 N. In contrast, when the load increased to 30 N, the wear coefficient rose as well, resulting in fewer, smoother wear scars on the composite's surface (Figure 13(f)). The tribooxide coating forms between sliding surfaces that reduces the wear coefficient when the load is increased to 50 N and forms a smooth surface (Figures 13(g) and 13(h)).

3.6. Surface Topography and Waviness. The surface topography and the surface roughness of the alloys after the tests were determined using a 3D profilometer and the same are shown in Figures 14–16. The alloys tested under dry conditions (Figures 14(a)–14(d)) yields surface roughness of 34.978 μm, 30.584 μm, 14.978 μm, and 12.584 μm at 20 N, 30 N, 40 N and 50 N load, respectively. Alloys under lubricated condition (Figures 15(a)–15(d)) presents surface roughness of 9.499 μm, 8.485 μm, 7.427 μm, and 5.409 μm at 20 N, 30 N, 40 N, and 50 N load, respectively. Whereas alloys under DLC-coated condition (Figures 16(a)–16(d)) results from surface roughness of 8.372 μm, 7.347 μm, 4.527 μm, and 4.377 μm at 20 N, 30 N, 40 N, and 50 N load, respectively.

From the results of surface roughness and topography it is understood that the surface roughness decreases as the applied load increases because of refined Si particle, lubrication, and DLC Coating offers less friction and wear. Comparing the surface roughness of alloys with coefficient of friction and wear coefficient under three test conditions, the results agrees.

4. Conclusions

The key conclusions drawn from the present investigation is as follows:

(i) Hypereutectic Al-Si24 alloy was successfully fabricated with a novel UVSS technique.

(ii) The Si granules refines and mixes homogeneously throughout the matrix.

(iii) Due to refinement of Si particle, the alloy yields enhancement in tensile strength.

(iv) The wear tests using linear reciprocating tribometer were successfully performed on the prepared alloys under three different conditions, and the results were obtained.

(v) The coefficient of friction and wear coefficient reduces with an increase in applied load under dry, lubricated, and coated conditions.

(vi) In comparison to the dry and lubricated states, the DLC-coated condition produces the lowest coefficients of friction, wear coefficients, and surface roughness. SAE20W40 engine oil significantly lowers the coefficient offriction (COF) and wear coefficients because of hard Si particles in the composite function as a solid lubricant in both dry and lubricated circumstances.

This investigation sheds light on the link between a–C: H coatings and sliding components in industrial and automotive applications.

Data Availability

The statement about where the data were generated and analysed during this study has been included in the manuscript in section materials and methods.

Conflicts of Interest

The authors declare that they have no conflicts of interest.

References

[1] J. E. Hatch, *Aluminium: Properties and Physical Metallurgy*, pp. 231-232, ASM, Metals Park, OH, USA, 1984.

[2] M. Warmuzek, "Aluminum-silicon casting alloys: an atlas of micro fractographs," *ASM international*, vol. 9, pp. 39–44, 2004.

[3] K. Mohammed Jasim and E. S. Dwarakadasa, "Wear in Al-Si alloys under dry sliding conditions," *Wear*, vol. 119, no. 1, pp. 119–130, 1987.

[4] H. Torabian, J. P. Pathak, and S. N. Tiwari, "Wear characteristics of Al-Si alloys," *Wear*, vol. 172, no. 1, pp. 49–58, 1994.

[5] P. J. Blau, *ASM Handbook: Friction, Lubrication, and Wear Technology*, ASM International Handbook Committee, New York, NY, USA, vol. 18, 1992

[6] A. S. Reddy, B. P. Bai, K. S. S. Murthy, and S. K. Biswas, "Wear and seizure of binary Al- Si alloys," *Wear*, vol. 171, no. 1-2, pp. 115–127, 1994.

[7] G. B. Narasimha, M. Vamsi Krishna, and R. Sindhu, "Prediction of wear behaviour of almg1sicu hybrid MMC using taguchi with grey rational analysis," *Procedia Engineering*, vol. 97, pp. 555–562, 2014.

[8] P. K. Rohatgi and B. C. Pai, "Effect of microstructure and mechanical properties on the seizure resistance of cast aluminium alloy," *Wear*, vol. 28, no. 3, pp. 353–367, 1974.

[9] K. G. Basava Kumar, "Influence of Refinement and modification on dry sliding wear behavior of hypereutectic Al-Si cast alloys," *Advanced Materials Research*, vol. 685, pp. 112–116, 2013.

[10] N. Nuraliza, S. Syahrullail, and M. H. Faizal, "Tribological properties of aluminum lubricated with palm olein at different load using pin-on-disk machine," *Jurnal Tribologi*, vol. 9, pp. 45–59, 2016.

[11] R. G. Guan, Z. Y. Zhao, C. S. Lee, Q. S. Zhang, and C. M. Liu, "Effect of wavelike sloping plate rheocasting on microstructures of hypereutectic Al-18 pct Si-5 pct Fe alloys," *Metallurgical and Materials Transactions B*, vol. 43, pp. 337–343, 2012.

[12] Q. Wang, L. Li, R. Zhou, X. Fan, and B. Geng, "Microstructures and wear behavior of the rheo-squeeze casting high silicon aluminium alloys pipe with the gradient structure," *Materials Research Express*, vol. 5, no. 10, Article ID 106505, 2018.

[13] Y. B. Zhang, J. C. Jie, Y. Gao, Y. P. Lu, and T. J. Li, "Effects of ultrasonic treatment on the formation of iron-containing intermetallic compounds in Al-12%Si-2%Fe alloys," *Intermetallics*, vol. 42, pp. 120–125, 2013.

[14] Y. Osawa, S. Takamori, T. Kimura, M. Kazumi, and K. Hideki, "Morphology of intermetallic compounds in Al-Si-Fe alloy and its control by ultrasonic vibration," *Materials Transactions*, vol. 48, no. 9, pp. 2467–2475, 2007.

[15] V. Tirth, S. Ray, and M. I. Kapoor, "Effect of squeeze pressure on aging and mechanical properties of AA2218-5 Wt pct Al2O3 (TiO2) composites," *Metallurgical and Materials Transactions A*, vol. 40, pp. 1246–1254, 2009.

[16] C. Lin, S. Wu, L. Shulin, P. An, and H. Wu, "Effects of high pressure rheo-squeeze casting on Fe-containing intermetallic compounds and mechanical properties of Al-17Si-2Fe-(0, 0.8) V alloys," *Materials Science and Engineering*, vol. 713, pp. 105–111, 2018.

[17] V. Tirth and A. Amir, "Effect of liquid forging pressure on solubility and freezing coefficients of cast aluminum 2124, 2218 and 6063 alloys," *Archives of Metallurgy and Materials*, vol. 65, no. 1, pp. 357–366, 2020.

[18] A. Edacherian, A. Ali, and V. Tirth, "Investigations of the tribological performance of A390 alloy hybrid aluminum matrix composite," *Materials*, vol. 11, no. 12, p. 2524, 2018.

[19] A. Khemraj, "Tribo-mechanical behavior of complex hypereutectic Al–Si alloy compressed through a converging die at elevated temperatures," *Materials Research Express*, vol. 5, no. 7, p. 6509, 2018.

[20] S. Mahato, T. Perry, A. Sachdev, and S. K. Biswas, "Role of silicon in resisting subsurface plastic deformation in tribology of aluminium–silicon alloys," *Tribology International*, vol. 43, no. 1-2, pp. 381–387, 2010.

[21] P. Kumar and M. F. Wani, "Effect of load on the tribological properties of hypereutectic Al–Si alloy under boundary lubrication conditions," *Materials Research Express*, vol. 4, no. 11, p. 6519, 2017.

[22] B. A. Khorramian, G. R. Iyer, S. Kodali, P. Natarajan, and R. Tupil, "Review of anti wear additives for crankcase oils," *Wear*, vol. 169, no. 1, pp. 87–95, 1993.

[23] S. Bhowmick and A. T. Alpas, "The performance of hydrogenated and non-hydrogenateddiamond-like carbon tool coatings during the dry drilling of 319 Al," *International Journal of Machine Tools and Manufacture*, vol. 48, no. 7-8, pp. 802–814, 2008.

[24] P. Kumar and M. F. Wani, "Friction and wear characterization of hypereutectic Al-Si alloy/steel tribopair under dry and lubricated conditions," *Jurnal Tribologi*, vol. 15, pp. 21–49, 2017.

[25] C. D. Erdemir, "Tribology of diamond-like carbon films: recent progress and future prospects," *Journal of Physics D: Applied Physics*, vol. 39, no. 18, pp. R311–R327, 2006.

[26] S. Bhowmick and A. T. Alpas, "Minimum quantity lubrication drilling of aluminium-silicon alloys in water using diamond-like carbon coated drills," *International Journal of Machine Tools and Manufacture*, vol. 48, no. 12-13, pp. 1429–1443, 2008.

[27] S. Bhowmick and A. T. Alpas, "The role of diamond-like carbon coated drills on minimum quantity lubrication drilling of magnesium alloys," *Surface and Coatings Technology*, vol. 205, no. 23-24, pp. 5302–5311, 2011.

[28] W. Ni, Y. T. Cheng, A. M. Weiner, and T. A. Perry, "Tribological behaviour of diamond-like-carbon (DLC) coatings against aluminium alloys at elevated temperatures," *Surface and Coatings Technology*, vol. 201, no. 6, pp. 3229–3234, 2006.

[29] W. S. Miller, L. Zhuang, J. Bottema et al., "Recent development in aluminium alloys for the automotive industry," *Materials Science and Engineering*, vol. 280, no. 1, pp. 37–49, 2000.

[30] J. R. Davis, "Friction and wear of internal combustion engine parts," in *ASM Handbook, Friction, Lubrication, and Wear*

Technology, vol. 18, pp. 553–562, no. 10, ASM International, Materials Park, OH, USA, 1992.

[31] E. Konca, Y. T. Cheng, A. M. Weiner, J. M. Dasch, and A. T. Alpas, "Elevated temperature tribological behavior of non-hydrogenateddiamond-like carbon coatings against 319 aluminum alloy," *Surface and Coatings Technology*, vol. 200, no. 12-13, pp. 3996–4005, 2006.

[32] D. Callegari, A. Marwick, and N. E. Lustig, "Thermal stability and electrical properties of hydrogenated amorphous carbon film," *Applied Physics Letters*, vol. 65, no. 25, pp. 3200–3202, 1994.

[33] K. Saijo, M. Yagi, K. Shibuki, and S. Takatsu, "The improvement of the adhesion strength of diamond films," *Surface and Coatings Technology*, vol. 43-44, pp. 30–40, 1990.

[34] H. Yoshikawa and A. Nishiyama, "CVD diamond coated insert for machining high silicon aluminum alloys," *Diamond and Related Materials*, vol. 8, no. 8-9, pp. 1527–1530, 1999.

[35] E. Liu, B. Blanpain, E. Dekempeneer, F. Loffler, J. P. Celis, and J. R. Roos, *Diamond Films and Technology*, vol. 4, pp. 37–49, 1994.

[36] S. Bhowmick, A. Banerji, and A. T. Alpas, "Tribological behaviour of Al-6.5%, -12%, -18.5% Si alloys during machining using CVD diamond and DLC coated tools," *Surface and Coatings Technology*, vol. 284, no. 25, pp. 353–364, 2015.

[37] Y. Bounouh, M. L. Theye, A. Dehbi-Alaoui, A. Matthews, and J. P. Stoquert, "Influence of annealing on the hydrogen bonding and the microstructure of diamondlike and polymerlike hydrogenated amorphous carbon films," *Physical Review B: Condensed Matter*, vol. 51, no. 15, pp. 9597–9605, 1995.

[38] N. D. Malleswararao, I. N. Niranjan Kumar, and B. Nagesh, "Friction and wear properties of rapid solidified H-Al-17Si alloys processed by UV assisted stir - squeeze casting with DLC-star (CrN + a-c:H) coating under HFRR," *Tribology in Industry*, vol. 42, no. 4, pp. 529–546, 2020.

[39] C. M. Chen, C. C. Yang, and C. G. Chao, "Dry sliding wear behaviours of Al–25Si–2.5 Cu–1Mg alloys prepared by powder thixocasting," *Materials Science and Engineering*, vol. 397, no. 1, pp. 178–189, 2005.

[40] N. D. Malleswararao and I. N. kumar, "Mechanical characterization of rapid solidified alsicumg alloys by new CRSS casting method under T6 condition," *International Journal of Innovative Technology and Exploring Engineering*, vol. 8, no. 12, pp. 2897–2902, 2019.

[41] N. Saheb, T. Laoui, A. R. Daud, M. Harun, S. Radiman, and R. Yahaya, "Influence of Ti addition on wear properties of Al-Si eutectic alloys," *Wear*, vol. 249, no. 8, pp. 656–662, 2001.

[42] J. David Raja Selvam, I. Dinaharan, and P. M. Mashinini, "High Temperature Sliding Wear Behavior of AA6061/fly Ash Aluminum Matrix Composites Prepared Using Compocasting Process, Tribology – Materials," *Surfaces & Interfaces*, vol. 11, no. 1, pp. 39 46, 2017.